LAWRENCE
LIVERMORE
NATIONAL
LABORATORY

UCRL-JRNL-227767

Electronic Spin Crossover of Iron in Ferroperclase in Earth#s Lower Mantle

J. F. Lin, G. Vanko, S. D. Jacobsen, V. Iota, V. V. Struzhkin, V. B. Prakapenka, A. Kuznetsov, C. S. Yoo

February 6, 2007

Science

Electronic Spin Crossover of Iron in Ferroperclase in Earth's Lower Mantle

Jung-Fu Lin[1], György Vankó[2], Steven D. Jacobsen[3], Valentin Iota-Herbei[1], Viktor V. Struzhkin[4], Vitali B. Prakapenka[5], Alexei Kuznetsov[5], Choong-Shik Yoo[1]

[1]*Lawrence Livermore National Laboratory, 7000 East Avenue, Livermore, CA 94550, USA*
[2]*European Synchrotron Radiation Facility, B.P. 220 F-38043 Grenoble Cedex 9, France*
[3]*Department of Earth and Planetary Sciences, Northwestern University, Evanston, IL 60208, USA*
[4]*Geophysical Laboratory, Carnegie Institution of Washington, 5251 Broad Branch Rd. NW, Washington, DC 20015*
[5]*Consortium for Advanced Radiation Sources, The University of Chicago, Chicago, IL 60637, USA*

Pressure-induced electronic spin-pairing transitions of iron and associated effects on the physical properties have been reported to occur in the lower-mantle ferropericlase, silicate perosvkite, and perhaps in post silicate perovskite at high pressures and room temperature[1-12]. These recent results are motivating geophysicists and geodynamicists to reevaluate the implications of spin transitions on the seismic heterogeneity, composition, as well as the stability of the thermal upwellings of the Earth's lower mantle[13-17]. Here we have measured the spin states of iron in ferropericlase and its crystal structure up to 95 GPa and 2000 K using a newly constructed X-ray emission spectroscopy and diffraction with the laser-heated diamond cell[18-20]. Our results show that an isosymmetric spin crossover occurs over a pressure-temperature range extending from the upper part to the lower part of the lower mantle[6,11,21], and low-spin ferropericlase likely exists in the lowermost mantle. Although continuous changes in physical and chemical

properties are expected to occur across the spin crossover, the spin crossover results in peculiar behavior in the thermal compression and sound velocities. Therefore, knowledge of the fraction of the spin states in the lower-mantle phases is thus essential to correctly evaluate the composition, geophysics, and dynamics of the Earth's lower mantle.

The nature of the spin-pairing transitions of iron in deep-mantle minerals at high temperatures has been based largely on theory, lacking experimental tests on the predicted geophysical and geochemical consequences[1-12]. Changes in the electronic structure of iron is thought to promote partitioning of iron into ferropericlase relative to perovskite[1] and nonconvecting layers in the lower mantle[2]; though, such conjecture has not been supported in recent experiments[7,22-23]. Recent theoretical calculations predict that the spin transition of Fe^{2+} in ferropericlase would occur continuously over an extended pressure range, thus more accurately referred to as a spin crossover, under the pressure-temperature conditions of the lower mantle[6,11]. In this case, the associated effects across a spin crossover in ferropericlase would be gradual, and therefore less likely to permit seismological detection. Conditions in the Earth's lower mantle vary from 22 to 140 GPa and temperatures of 1800 K to 4000 K (ref. 21). An experimental determination of the high-temperature effect on the spin transitions of lower-mantle phases is therefore essential to reliably imply the effects of the spin transitions to the Earth's interior. Here we have studied the electronic spin states of iron in ferropericlase [$(Mg_{0.75},Fe_{0.25})O$] and its crystal structure under relevant lower-mantle conditions using newly interfaced X-ray emission spectroscopy (XES)[18-20] and X-ray diffraction systems with a laser-heated diamond cell (LHDAC)[18], and we discuss the consequences of the observed spin crossover on the geophysics and geodynamics of the Earth's lower mantle.

The spin states of iron in single crystal $(Mg_{0.75},Fe_{0.25})O$ at high pressures and temperatures were probed by *in situ* XES and diffraction in a LHDAC. The samples were pre-oriented <110> crystal plates or polycrystalline samples of $(Mg_{0.75},Fe_{0.25})O$ composition[5] measuring approximately 12 μm thick and 70 μm in diameter. Samples were loaded into diamond cells with Be gaskets and boron or cubic BN gasket inserts. Dried NaCl layers acted as the thermal insulators between the sample and diamond anvils, as well as the pressure medium, and pressure calibrant[24].

A Rowland circle spectrometer with a one-meter diameter in the vertical scattering geometry was configured around the double-sided laser-heating system at the GSECARS sector of the Advanced Photon Source (APS), Argonne National Laboratory (ANL) for XES of iron in the sample under high pressures and temperatures. A monochromatic X-ray beam of 14 keV was focused down to approximately 5 μm vertically and horizontally at the sample position, and a Nd:YLF laser of 25 μm in diameter at the sample position, operating in continuous donut mode (TEM_{01}), was used to laser heat the sample from both sides of the DAC. The Fe-K_{β} emission spectra were collected by a silicon detector through the Be gasket and a Si (333) analyzer in the Rowland circle geometry. During the laser-heating experiments, the energy of the monochromatic X-ray can be adjusted to higher energy to allow collecting X-ray diffraction patterns by an image plate (MAR345). The counting time for each XES spectrum was about thirty minutes and typically ten spectra were continuously collected at the same pressure and temperature and co-added. Care was taken to ensure that the X-ray and laser beams were aligned and the sample position remained intact during the course of the long-term heating. Greybody temperatures were determined by fitting the thermal radiation spectrum between 670 nm and 830 nm to the Planck radiation function. Temperatures were limited to 2000 K and below to avoid other technical difficulties in the experiments, and temperature uncertainties were approximately 100 to 150 K. Pressures were determined from the ruby spheres next to the sample and/or the NaCl pressure scale[24]. The details of the experimental set-up and sample syntheses are reported elsewhere[5,9,18].

The XES spectra of the Fe K_β fluorescence lines in $(Mg_{0.75},Fe_{0.25})O$ were collected up to 95 GPa and 2000 K, and X-ray diffraction patterns were collected from some of the samples before, during, and after laser heating at high pressures (Figs. 1, 2). The appearance and disappearance of the K_β' satellite peak as well as the energy shift of ~1.6 eV in the K_β main peak in the XES spectra reveal a high-spin to low-spin transition of iron in the sample at high pressures and temperatures (Fig. 1)[5]; however, the Fe K_β spectrum arises from multiplet electronic transitions with varying line widths and the determination of the 3d spin momentum from the spectrum is nontrivial[19,20].

To quantitatively derive the 3d spin momentum and the fraction of the high-spin and low-spin states, the XES spectra are analyzed using the line shape analyses by integrating the absolute values of the difference spectra and comparing these integrals to that obtained on references (hereafter called the IAD analyses) (Fig. 1,3)[18,20]. The IAD analyses use the information of the full Fe K_β spectrum and are model independent. It has been shown that the derived IAD values linearly correlate with the spin momentum and provide a reliable method for determining the fraction of the high-spin and low-spin states in the sample[19,20].

The derived fractions of the high-spin and low-spin states are used to construct the spin crossover phase diagram of iron in $(Mg_{0.75},Fe_{0.25})O$ up to 95 GPa and 2000 K (Figs. 3,4). While high temperatures do not significantly affect the ratio of the high-spin to low-spin states below 50 GPa and at 95 GPa, much stronger temperature effects on the spin crossover are observed between approximately 50 GPa to 80 GPa. The high-spin to low-spin transition clearly widens with increasing temperatures at high pressures, and a spin crossover is observed to occur over a wide pressure-temperature range (Fig. 4).

While the XES results reveal a continuous spin crossover with a mixed population of high-spin and low-spin states of iron in ferropericlase at high pressures and temperatures, X-ray diffraction patterns show that the $(Mg_{0.75},Fe_{0.25})O$ sample is stable in the B1 structure before, during, and after the experiments up to 95 GPa and 2000 K (ref. 25,26). Previous high-pressure and room-temperature experiments showed that low-spin and high-spin states have unique physical properties, such as volume, incompressibility, and sound velocities, and can be categorized as two distinct phases, high-spin ferropericlase and low-spin ferropericlase[5,7,9]. Based on our current XES and diffraction results, the isosymmetric spin crossover in the ferropericlase involves fast flipping of the 3d electrons with a mixed population of high-spin and low-spin states[6,11] in the same composition, though it remains to be seen if a phase separation would occur with high FeO contain in (Mg,Fe)O.

The spin crossover of iron in the lower-mantle phases significantly affects its implications for the geophysics and geodynamics of the Earth's lower mantle. Although the temperature effect on the spin transitions in the silicate perovskite is yet to be studied[2-4,8,12], the observed spin crossover in ferropericlase is anticipated as a general phenomenon that should also occur in silicate perovskite and post perovskite. Despite the dramatic changes in incompressibility, sound velocities, and radiative thermal conductivity across the spin transition at high pressures and room temperature[5,7,9], the spin transitions and associated changes in physical and chemical properties should occur quite continuously in the mantle. The continuous nature of the spin crossover observed here explains why no significant change in iron partitioning between ferropericlase and perovskite has been observed in recent high pressure-temperature experiments with a pyrolitic and olivine composition[22-23], as opposed to a proposed dramatic change in partitioning and chemical layering in the lower mantle[1-2].

Comparison to the model geotherm of the Earth's lower mantle[21] indicates that the high-spin to low-spin crossover of iron likely occurs from the upper part to the lower part of the lower mantle and that the low-spin ferropericlase exists in the lowermost mantle, i.e. at depth below ~2200 km. Hence, the sound velocities, transport properties, and other thermodynamic properties of the low-spin ferropericlase need to be considered in future geophysical and geochemical models in determining mineralogy and geodynamics of the lowermost mantle. In particular, the low-spin ferropericlase exhibits lower radiative thermal conductivity than the high-spin ferropericlase[7], and a spin crossover in ferropericlase would result in a continuously reduced radiative thermal conductivity of ferropericlase from the upper part to the lower part of the lower mantle. The reduced radiative thermal conductivity of the low-spin ferropericlase is at odd to what is required for sustaining superplumes with sufficiently strong thermal conductivity in the lower mantle, affecting the understanding of the convective flow, the size, and the stability of the thermal upwellings in the lower mantle[16-17,27]. The relatively low creep strength and large elastic anisotropy of ferropericlase, as the second most constituent of Earth's lower mantle, are believed to play very important role in the viscosity, dynamics, and seismic anisotropy of the lower mantle[28-29]. Although the viscosity of the low-spin ferropericlase remains to be studied, recent high-pressure results showed that the low-spin ferropericlase is much stiffer and has much higher shear modulus than the high-spin ferropericlase. Such changes indicate that the viscosity of the low-spin ferropericlase likely differs from that of the high-spin ferropericlase, suggesting that the spin crossover can continuously change the rheology of the lower mantle.

Abnormal effects of the spin transition on the volume, incompressibility, and sound velocities of ferropericlase have been observed under high pressures and room temperatures; a decrease in volume and jumps in incompressibility and sound velocities are reported to occur at high pressures and room temperature[5,9]. As the temperature increases, these abnormal effects are expected to be reduced as ferropericlase with mixed spin states becomes more normal. Such transition from abnormal to normal behavior, however, can result in peculiar effects on physical properties of ferropericlase at high pressures and temperatures. In particular, the thermal compression curve and sound velocities of ferropericlase will be continuously influenced by the ratio of the high-spin and low-spin states, making the use of the classical equations of state with lattice finite strain theory unreliable to model the compression behavior across the spin crossover[24,30]. On the other hand, negligible (or even positive) temperature effect on the sound velocities may occur at the spin crossover pressures because of the change of the population of the spin states. That is, knowing the ratio of the high-spin to low-spin states in ferropericlase as well as in the silicate perovskite will be essential to correctly evaluate the composition, geophysics, and dynamics of the Earth's lower mantle.

1. Badro, J. *et al.* Iron partitioning in Earth's mantle: toward a deep lower mantle discontinuity. *Science* **300**, 789-791 (2003).
2. Badro, J. *et al.* Electronic transitions in perovskite: possible nonconvecting layers in the lower mantle. *Science* **305**, 383-386 (2004).
3. Li, J. *et al.* Electronic spin state of iron in lower mantle perovskite. *Proc. Natl. Acad. Sci. U.S.A.* **101**, 14027–14030 (2004).
4. Jackson, J. M. *et al.* A synchrotron Mössbauer spectroscopy study of (Mg,Fe)SiO_3 perovskite up to 120 GPa. *Amer. Miner.* **90**, 199-205 (2005).
5. Lin, J. F. *et al.* Spin transition of iron in magnesiowüstite in Earth's lower mantle. *Nature* **436**, 377-380 (2005).
6. Sturhahn, W., Jackson, J. M., & Lin, J. F. The spin state of iron in Earth's lower mantle minerals. *Geophys. Res. Lett.* **32**, L12307 (2005).
7. Goncharov, A. F., Struzhkin, V. V., & Jacobsen, S. D. Reduced radiative conductivity of low-spin (Mg,Fe)O in the lower mantle. *Science* **312**, 1205-1208 (2006).
8. Hofmeister, A. M. Is low-spin Fe^{2+} present in Earth's mantle? *Earth Planet. Sci. Lett.* **243**, 44-52 (2006).
9. Lin, J.F. *et al*. Sound velocities of ferropericlase in Earth's lower mantle. *Geophys. Res. Lett*. **33**, L22304, doi:10.1029/2006GL028099 (2006).

10. Persson, K., Bengtson, A., Ceder, G., & Morgan, D. *Ab initio* study of the composition dependence of the pressure-induced spin transition in the $(Mg_{1-x},Fe_x)O$ system, *Geophys. Res. Lett.* **33**, L16306 (2006).

11. Tsuchiya, T., Wentzcovitch, R. M., da Silva, C. R. S., & de Gironcoli S. Spin transition in magnesiowüstite in Earth's lower mantle. *Phys. Rev. Lett.* **96**, 198501 (2006).

12. Zhang, F. & Oganov, A. R. Valence state and spin transitions of iron in Earth's mantle silicates, *Earth Planet. Sci. Lett.* **249**, 436-43 (2006).

13. Kellogg, L. H., Hager, B. H., & van der Hilst, R. D. Compositional stratification in the deep mantle. *Science* **283**, 1881-1884 (1999).

14. van der Hilst, R. D., & Kárason, H. Compositional heterogeneity in the bottom 1000 kilometers of Earth's mantle: toward a hybrid convection model. *Science* **283**, 1885-1888 (1999).

15. Trampert, J., Deschamps, F., Resovsky, J., & Yuen, D. Probabilistic tomography maps chemical heterogeneities throughout the lower mantle. *Science* **306**, 853-856, (2004).

16. Matyska, C. & Yuen, D. A. Lower mantle dynamics with the post-perovskite phase change, radiative thermal conductivity, temperature- and depth-dependent viscosity, *Earth Planet. Sc. Lett.* **154**, 196-207 (2006).

17. Naliboff, J. B. & Kellogg, L. H. Dynamical effects of a step-wise increase in thermal conductivity and viscosity in the lowermost mantle. *Geophys. Res. Lett.* **33**, L12S09 (2006).

18. Lin, J. F. *et al.* X-ray emission spectroscopy in a laser-heated diamond anvil cell: probing spin state of transition metals in the Earth's interior. *J. Synchrotron Rad.* **12**, 637-641 (2005).

19. Vankó, G., Rueff, J.-P., Mattila, A., Nemeth, Z., & Shukla, A. Temperature- and pressure-induced spin-state transitions in $LaCoO_3$. *Phys. Rev.. B* **73**, 024424 (2006).

20. Vankó, G. *et al.* Probing the 3d spin momentum with X-ray emission spectroscopy: the case of molecular-spin transitions. *J. Phys. Chem. B* **110**, 11647-11653 (2006).

21. Brown, J. M. & Shankland, T. J. Thermodynamic parameters in the Earth as determined from seismic profiles. *Geophys. J. R. Astr. Soc.* **66**, 579-596 (1981).

22. Kobayashi, Y. *et al*. Fe-Mg partitioning between $(Mg,Fe)SiO_3$ post-perovskite, and magnesiumwüstite in the Earth's lower mantle. *Geophys. Res. Lett.* **32**, L19302 (2005).

23. Murakami, M., Hirose, K., Sata, N., & Ohishi, Y. Post-perovskite transition and mineral chemistry in the pyrolite lowermost mantle. *Geophys. Res. Lett.* **32**, L03304 (2005).

24. Birch, F. Equation of state and thermodynamic parameters of NaCl to 300 kbar in the high-temperature domain. *J. Geophys. Res.* **91**, 4949-4954 (1986).

25. Dubrovinski, L. S. *et al.* Stability of ferropericlase in the lower mantle. *Science* **289**, 430-432 (2000).

26. Lin, J. F. *et al.* Stability of magnesiowüstite in the Earth's lower mantle. *Proc. Natl. Acad. Sci. U.S.A.* **100**, 4405–4408 (2003).

27. Hofmeister, A. M. Mantle values of thermal conductivity and the geotherm from phonon lifetime. *Science* **283**, 1699–1706 (1999).

28. Karato, S. I. Plasticity-crystal structure systematics in dense oxides and its implications for the creep strength of the Earth's deep interior: a preliminary result. *Phys. Earth Planet. Inter.* **55**, 234-240 (1989).

29. Yamazaki, D. & Karato, S. I. Fabric development in (Mg,Fe)O during large strain, shear deformation: implications for seismic anisotropy in Earth's lower mantle. *Phys. Earth Planet. Inter.* **131**, 251-267 (2002).

30. Davies, G. F. & Dziewonski, A. M. Homogeneity and constitution of the Earth's lower mantle and outer core. *Phys. Earth Planet. Int.* **10**, 336-343, (1975).

Supplementary information is available on Nature's World-wide web site (http://www.nature.com) or as paper copy from the London editorial office of Nature

Acknowledgments

We acknowledge GSECARS and HPCAT, APS, ANL for the use of the synchrotron and laser facilities. We thank F. de Groot, J.-P. Rueff, and W. Sturhahn for helpful discussions and G. Shen and M. Hu for their assistance in the experiments. This work and use of the APS are supported by U.S. DOE, Basic Energy Sciences, Office of Science, under contract No. W-31-109-ENG-38, and the State of Illinois under HECA. This work at LLNL was performed under the auspices of the U.S. DOE by University of California and LLNL under Contract No. W-7405-Eng-48. J.F.L. is also supported by Lawrence Livermore Fellowship. S.D.J. acknowledges financial support from NSF/EAR 0440112 and V.V.S. acknowledges financial support from DOE.

Correspondence and requests for materials should be addressed to J.-F.L (e-mail: lin24@llnl.gov).

Figure 1 Representative X-ray emission spectra of Fe-K_β collected from ferropericlase-$(Mg_{0.75},Fe_{0.25})O$ at high pressures and temperatures. Upper panel, ~51 GPa and high temperatures; lower panel, ~80 GPa and high temperatures. High-quality XES spectra collected at 0 GPa and approximately 80 GPa are used as references for the IAD analyses[19,20] of the high-spin and low-spin states, respectively. Differences from the low-spin line shape are also shown below the spectra and used to derive the ratio of the high-spin to low-spin states in the sample. An energy shift of ~1.6 eV in the main emission peak (K_β) can also be seen across the spin transition. The high-spin to low-spin transition is found to be ready reversible in temperatures.

Figure 2 Representative angle-dispersive X-ray diffraction patterns of $(Mg_{0.75},Fe_{0.25})O$ at ~84 GPa and high temperatures collected from a laser-heated diamond cell. A monochromatic beam of 0.3344 Å in wavelength was used as the X-ray source and the diffracted X-rays were collected by an image plate (MAR345). The diffraction patterns were integrated with the FIT2D program, and the backgrounds were subtracted for clarity. $(Mg_{0.75},Fe_{0.25})O$ is stable in the B1 structure up to 1900 K and remains in the B1 structure after hours of laser heating[25,26]. Fp, $(Mg_{0.75},Fe_{0.25})O$; B2, NaCl thermal insulator in the B2 structure. Temperature uncertainties in the experiments were approximately 100 to 150 K. Optical observation of the laser-heated sample also shows no evidence of a phase separation.

Figure 3 Ratios of the high-spin iron in $(Mg_{0.75},Fe_{0.25})O$ at high pressures and temperatures. The high-spin ratio, γ_{HS}, is derived from the line shape analyses of the X-ray emission spectra[18,20] collected at high pressures and temperatures (Fig. 1). The large error bars at 47 GPa and 1300 K arise from the low statistics of the XES spectrum.

Figure 4 Isosymmetric spin crossover of Fe^{2+} in $(Mg_{0.75},Fe_{0.25})O$. The phase diagram is constructed from the derived ratio of the high-spin to low-spin states in the sample (Fig. 3). The vertical column on the right represents the colors for the ratios of the high-spin state, γ_{HS}, in the sample. The high-spin to low-spin crossover widens with increasing temperatures, and high temperatures have much stronger effects on the spin crossover between approximately 50 GPa to 80 GPa.

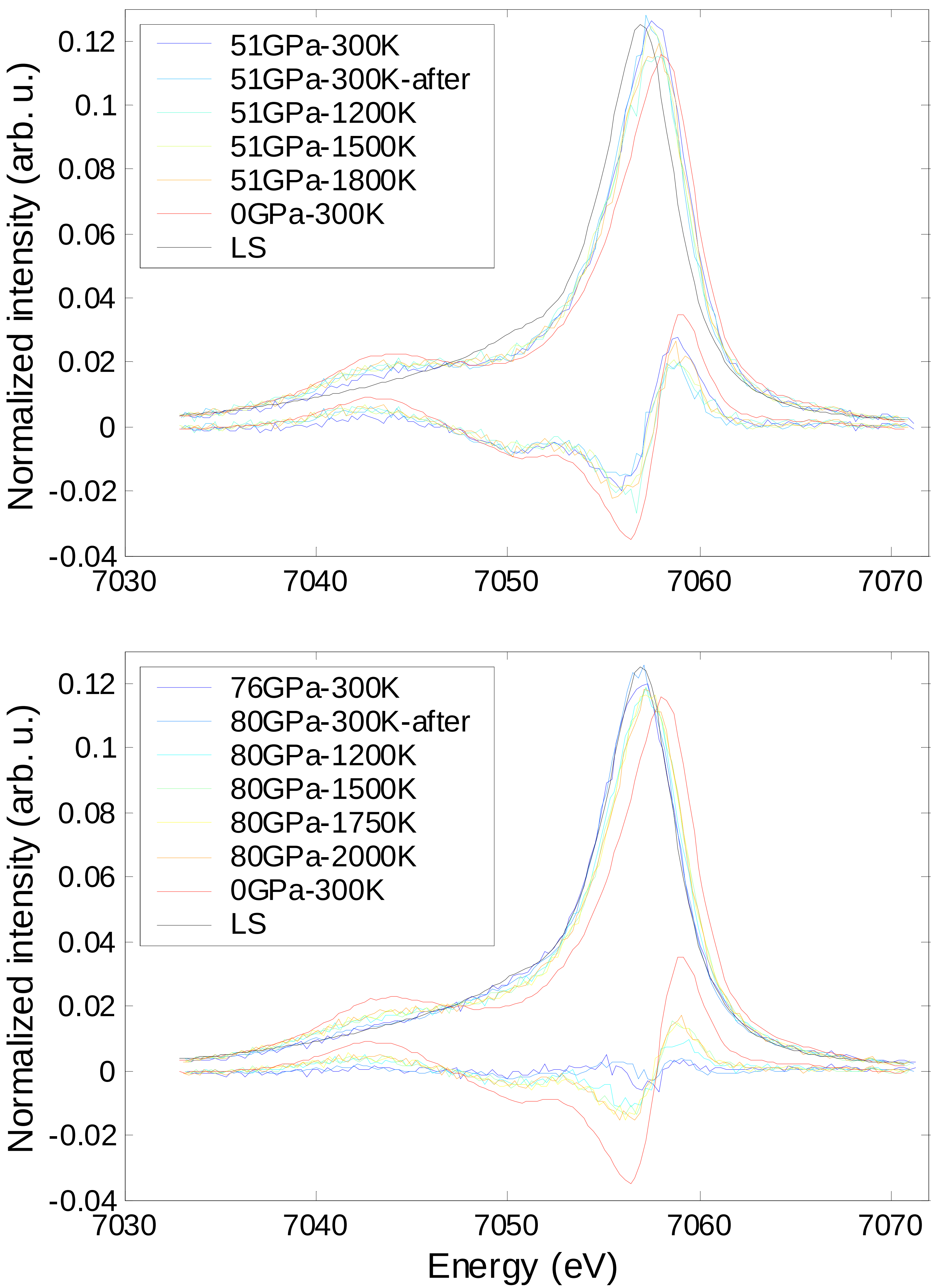

51GPa-300K
51GPa-300K-after
51GPa-1200K
51GPa-1500K
51GPa-1800K
0GPa-300K
LS
Normalized intensity (arb. u.)
0.12
0.1
0.08
0.06
0.04
0.02
0
-0.02
-0.04
7030
7040
7050
7060
7070
76GPa-300K
80GPa-300K-after
80GPa-1200K
80GPa-1500K
80GPa-1750K
80GPa-2000K
0GPa-300K
LS
Energy (eV)

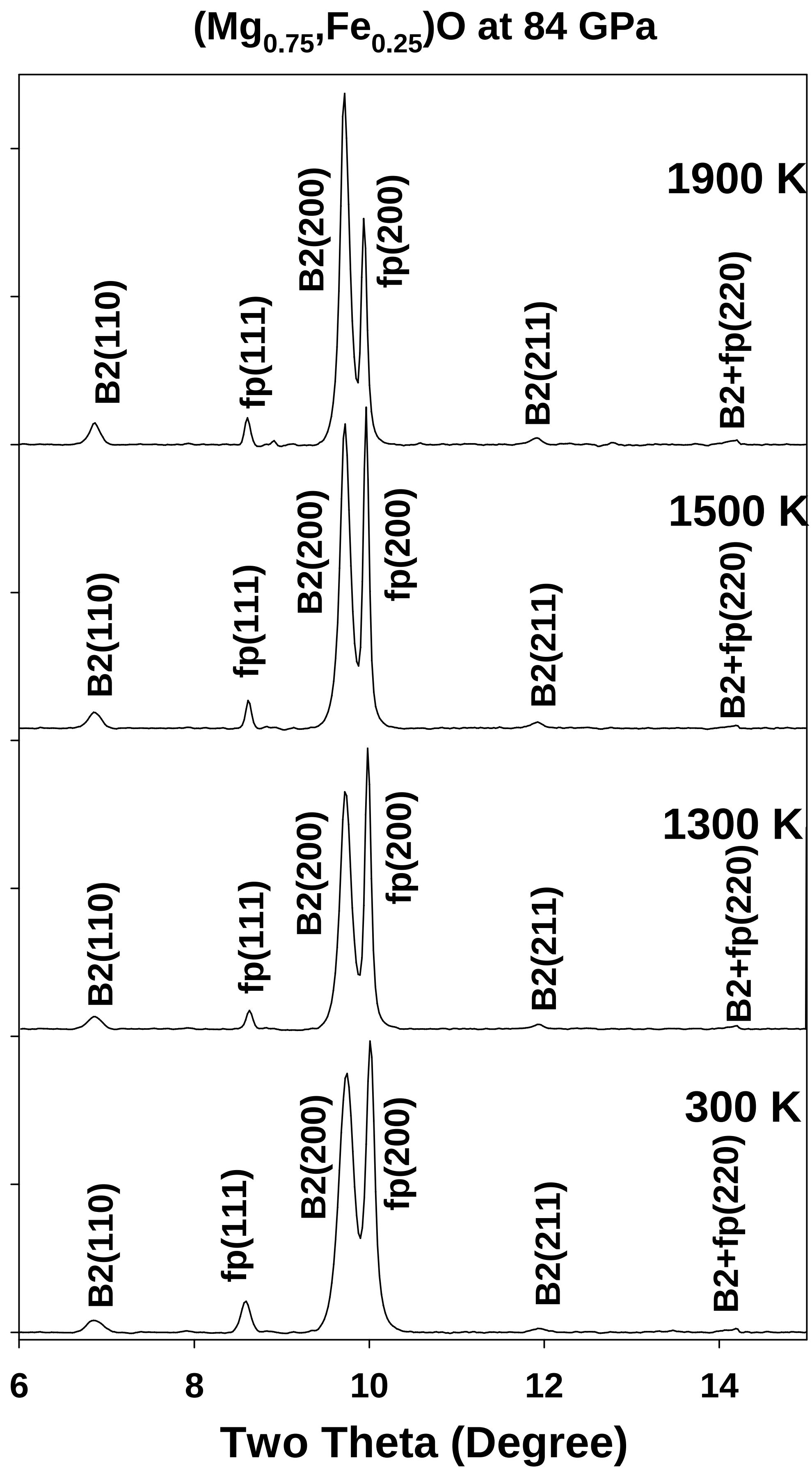

(Mg0.75,Fe0.25)O at 84 GPa
1900 K
1500 K
1300 K
300 K
B2(110)
fp(111)
B2(200)
fp(200)
B2(211)
B2+fp(220)
6
8
10
12
14
Two Theta (Degree)

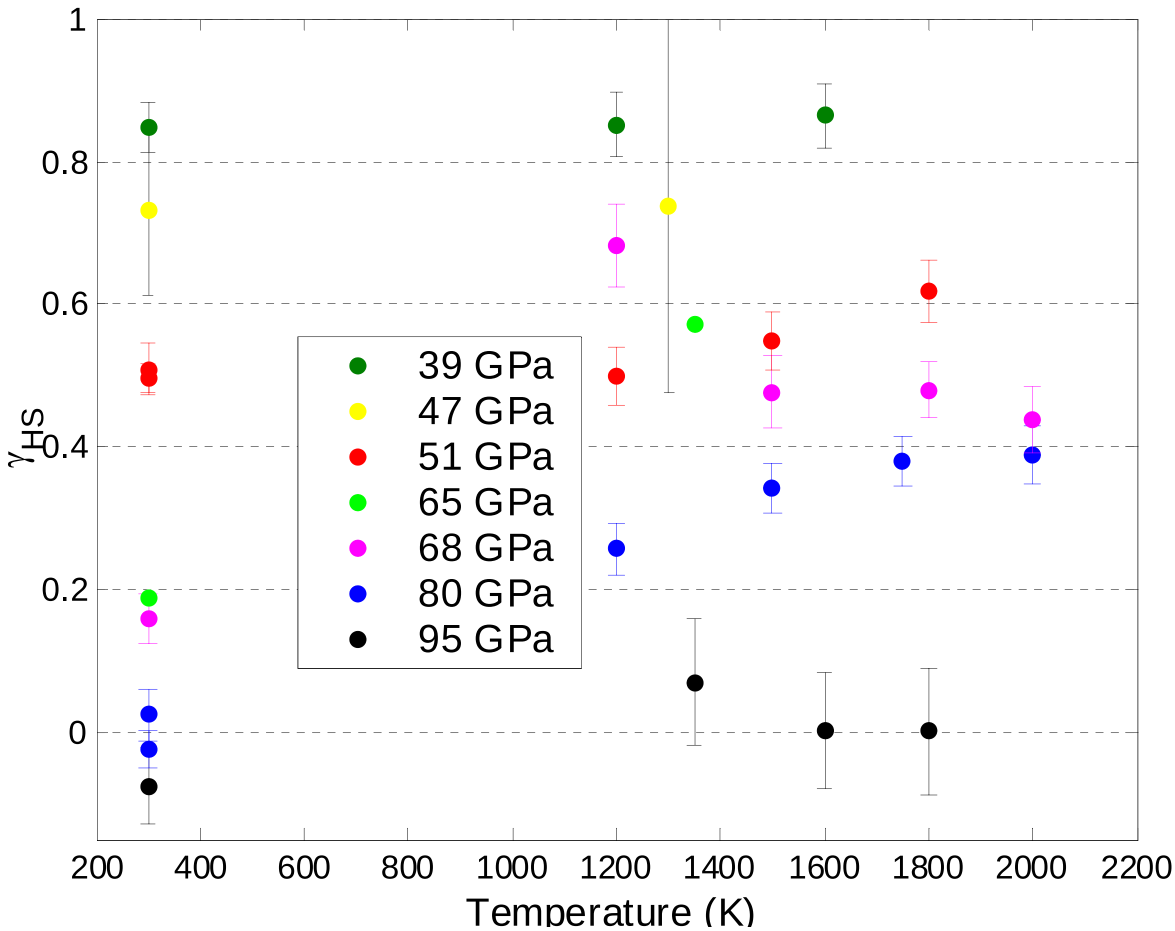

1
0.8
0.6
0.4
0.2
0
γ_{HS}
39 GPa
47 GPa
51 GPa
65 GPa
68 GPa
80 GPa
95 GPa
200
400
600
800
1000
1200
1400
1600
1800
2000
2200
Temperature (K)

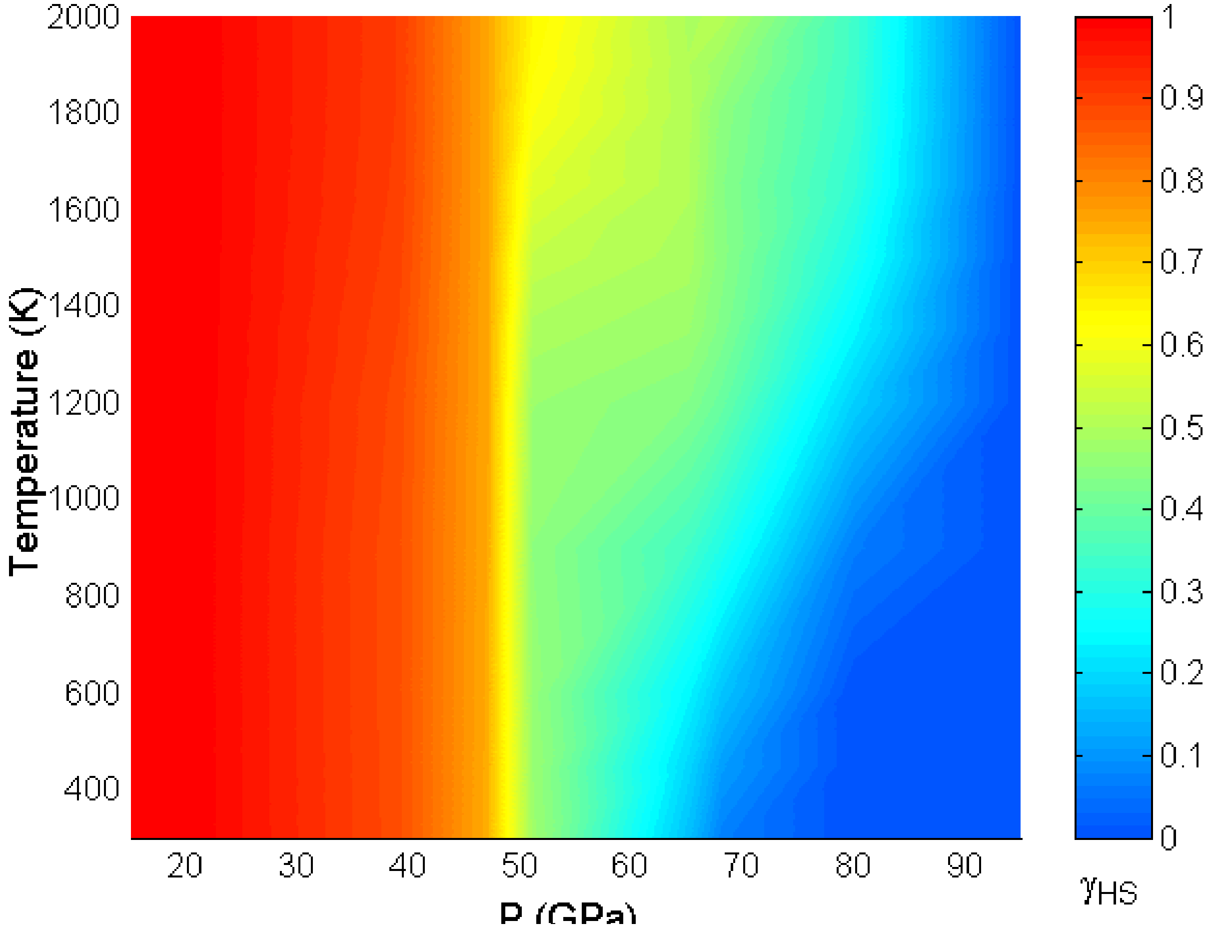

2000
1800
1600
1400
1200
1000
800
600
400
Temperature (K)
20
30
40
50
60
70
80
90
1
0.9
0.8
0.7
0.6
0.5
0.4
0.3
0.2
0.1
0
γ_{HS}